

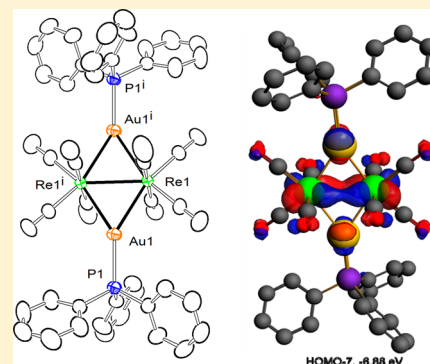
Studies of the Structures and Bonding of Gold-Bridged Dirhenium Carbonyl Cluster Complexes

Richard D. Adams,* Yuen Onn Wong, and Qiang Zhang

Department of Chemistry and Biochemistry, University of South Carolina, Columbia, South Carolina 29208, United States

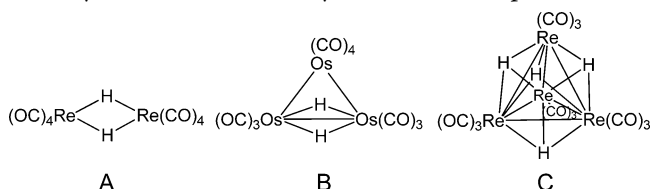
Supporting Information

ABSTRACT: The compounds $\text{Re}_2(\text{CO})_8(\mu\text{-AuPPh}_3)_2$, **1**, a dimer of $\text{Re}(\text{CO})_4(\mu\text{-AuPPh}_3)$, and $\text{ax,ax-Re}_2(\text{CO})_8(\text{PPh}_3)_2$ were obtained from UV–vis radiation-induced decarbonylation of the compound $\text{Re}(\text{CO})_5[\text{Au}(\text{PPh}_3)]$. Compound **1** contains two rhenium atoms bridged by two AuPPh_3 groups. The complex has 32 valence electrons and is formally unsaturated by the amount of two electrons. The Re–Re bond distance in **1** is unusually short (Re–Re = 2.9070(3) Å), as found by a single-crystal structural analysis. The nature of the metal–metal bonding in **1** was investigated by DFT computational analyses, which have provided evidence not only for σ -bonding but also significant complementary π -bonding directly between the two rhenium atoms. The electronic structure of $\text{Re}_2(\text{CO})_8(\mu\text{-H})_2$, **2**, was similarly analyzed and is compared with that of **1**. Compound **1** is intensely colored due to low-energy, metal-based electronic transitions between the HOMO and HOMO-2 and the LUMO. Compound **1** reacts with I_2 to yield $\text{Re}_2(\text{CO})_8(\mu\text{-AuPPh}_3)(\mu\text{-I})$, **3**, and the known compound $\text{Re}_2(\text{CO})_8(\mu\text{-I})_2$, **4**, by substitution of the bridging AuPPh_3 groups with bridging iodide ligands. Compound **3** is electronically saturated, 34 valence electrons, and contains a formal Re–Re single bond: Re–Re = 3.2067(5) Å. Compound **3** was also in a high yield (83%) from the reaction of $\text{Re}_2(\text{CO})_8(\mu\text{-H})(\mu\text{-CH=CHC}_4\text{H}_9)$ with $\text{Au}(\text{PPh}_3)\text{I}$. The Re–Re bonding in compounds **3**, **4**, and $\text{Re}_2(\text{CO})_{10}$ was also analyzed computationally, and this bonding was compared with their bonding in **1** and **2**.



INTRODUCTION

The similarities between the hydrogen atom and the $\text{Au}(\text{PPh}_3)$ group are well-known.¹ The two species are effectively isolobal and both contain only one valence electron. H and the $\text{Au}(\text{PPh}_3)$ group are well-known to bridge metal–metal bonds effectively in polynuclear metal complexes.^{2,3} There are a number of hydride-bridged metal carbonyl cluster complexes, such as $\text{Re}_2(\text{CO})_8(\mu\text{-H})_2$, **A**,⁴ $\text{Os}_3(\text{CO})_{10}(\mu\text{-H})_2$, **B**,⁵ $\text{Re}_4(\text{CO})_{12}(\mu\text{-H})_4$, **C**, and higher nuclearity cluster complexes, such as $\text{Pt}_2\text{Re}_3(\text{CO})_9(\text{P-}t\text{-Bu}_3)_3(\mu\text{-H})_6$,⁷ and $[\text{Ru}_3(\text{CO})_8(\mu_3\text{-CMe})(\mu\text{-H})_2(\mu_3\text{-H})]_2$,⁸ that have attracted interest because they are formally electronically unsaturated. Unsaturated metal cluster complexes are of interest because they exhibit higher reactivity than their electronically saturated counterparts.^{7–10}



A few unsaturated triosmium carbonyl cluster complexes containing the bridging $\text{Au}(\text{PR}_3)$ group(s) have also been prepared (e.g., $\text{Os}_3(\text{CO})_{10}(\mu\text{-AuPPh}_3)_2$,¹¹ $\text{Os}_3(\text{CO})_{10}(\mu\text{-AuPPh}_3)(\mu\text{-H})$,¹² and $\text{Os}_3(\text{CO})_{10}(\mu\text{-AuPPh}_3)(\mu\text{-Ph})$ ¹³) that are related to $\text{Os}_3(\text{CO})_{10}(\mu\text{-H})_2$.

We have now prepared and characterized the new dirhenium complex $\text{Re}_2(\text{CO})_8(\mu\text{-AuPPh}_3)_2$, **1**, that contains two bridging

$\text{Au}(\text{PPh}_3)$ groups. The two rhenium atoms contain a total of 32 valence electrons, leaving the metal atoms formally unsaturated by the amount of two electrons. In accord with this, the Re–Re distance in **1** is unusually short. The metal–metal bonding in **1** was investigated by DFT computational analyses, which have provided evidence for strong bonding directly between the two rhenium atoms. For comparisons, the electronic structure of $\text{Re}_2(\text{CO})_8(\mu\text{-H})_2$, **2**, was also investigated. Reactions of **1** with I_2 were investigated and were found to provide the new electronically saturated compound $\text{Re}_2(\text{CO})_8(\mu\text{-AuPPh}_3)(\mu\text{-I})$, **3**, and the previously reported complex $\text{Re}_2(\text{CO})_8(\mu\text{-I})_2$, **4**.¹⁴ Compound **3** was prepared independently in a high yield from the reaction of $\text{Re}_2(\text{CO})_8(\mu\text{-H})(\mu\text{-CH=CHC}_4\text{H}_9)$ with $\text{Au}(\text{PPh}_3)\text{I}$. The Re–Re bonding in **3** and **4** was also investigated by computational methods. Details of these studies are provided in this report.

EXPERIMENTAL SECTION

General Data. Reagent grade solvents were dried by the standard procedures and were freshly distilled prior to use. Infrared spectra were recorded on a Thermo Nicolet Avatar 360 FT-IR spectrophotometer. Room-temperature ^1H NMR and $^{31}\text{P}\{^1\text{H}\}$ NMR were recorded on a Bruker Avance/DRX 400 NMR spectrometer operating at 400.3 and 162.0 MHz, respectively. Positive/negative ion mass spectra were recorded on a Micromass Q-TOF instrument by using electrospray (ES) ionization or electron impact (EI) ionization. UV–vis spectra

Received: October 15, 2013

were recorded on a (Agilent/Varian Cary 50) UV–vis spectrometer in methylene chloride solvent at a concentration of 0.46×10^{-4} M. $\text{Re}(\text{CO})_5(\text{AuPPh}_3)_2$,¹⁵ $\text{Re}_2(\text{CO})_8(\mu\text{-H})(\mu\text{-CH=CHC}_4\text{H}_9)_2$,¹⁶ and $\text{Au}(\text{PPh}_3)_3$ ¹⁷ were prepared by the previously reported procedures. Product separations were performed by TLC in air on Analtech 0.25 mm silica gel 60 Å F254 glass plates.

Synthesis of $\text{Re}_2(\text{CO})_8(\mu\text{-AuPPh}_3)_2$, 1. A 45.0 mg (0.0572 mmol) portion of $\text{Re}(\text{CO})_5\text{Au}(\text{PPh}_3)$ was dissolved in 25 mL of benzene and irradiated for 30 min, and the solution turned to brown. The solvent was removed in vacuo. The residue was separated by TLC by using a 4:1 hexane/methylene chloride (v/v) solvent mixture to yield in order of elution: (1) a colorless band of $\text{Re}_2(\text{CO})_{10}$, 0.7 mg (4% yield), (2) a colorless band identified as $\text{Re}_2(\text{CO})_8(\text{PPh}_3)_2$,¹⁶ 6.7 mg (21% yield), and (3) a red band of $\text{Re}_2(\text{CO})_8(\mu\text{-AuPPh}_3)_2$, 1, 7.6 mg (18% yield). Spectral data for 1: IR ν_{CO} (cm^{-1} in methylene chloride): 2065(w), 2028(s), 1976(vs), 1942(m), 1917(s). ^1H NMR (CD_2Cl_2 , in ppm): δ = 7.20–7.36 (m, 30H, Ph). ^{31}P NMR (CD_2Cl_2 , in ppm): δ = 76.17 (s). Mass Spec. EI/MS m/z : 1514, M^+ , 1486, $\text{M}^+ - \text{CO}$. The isotope distribution pattern is consistent with the presence of two gold atoms and two rhenium atoms. The UV–vis absorption spectrum in CH_2Cl_2 solvent: λ_{max} = 327 nm, ϵ = 6692 $\text{cm}^{-1} \text{M}^{-1}$, λ_{max} = 420 nm, ϵ = 2820 $\text{cm}^{-1} \text{M}^{-1}$, and λ_{max} = 493 nm, ϵ = 5836 $\text{cm}^{-1} \text{M}^{-1}$.

Synthesis of $\text{Re}_2(\text{CO})_8(\mu\text{-AuPPh}_3)(\mu\text{-I})$, 3. A 3.2 mg (0.0126 mmol) portion of I_2 was added to 19.0 mg (0.0125 mmol) of 1 in 10 mL of benzene. The solution was stirred at room temperature for 15 min. During this time, the solution turned from orange to yellow. The solvent was removed in vacuo, and the products were separated by TLC by using a 4:1 (v/v) hexane/methylene chloride solvent mixture to yield in order of elution: (1) a yellow band of $\text{Re}_2(\text{CO})_8(\mu\text{-AuPPh}_3)(\mu\text{-I})$, 3, (13% yield), and (2) a colorless band of $\text{Au}(\text{PPh}_3)_3$, 4.9 mg (33% yield). Spectral data for 3: IR ν_{CO} (cm^{-1} in methylene chloride): 2094(w), 2064(m), 2005(s), 1972(m), 1935(m). ^{31}P NMR (CD_2Cl_2 , in ppm): δ = 76.79 (s). Mass Spec. EI/MS m/z : 1182, M^+ , 1154, $\text{M}^+ - \text{CO}$. The isotope distribution pattern is consistent with the presence of one gold atom and two rhenium atoms.

Alternative Synthesis of 3. A 45.0 mg (0.0661 mmol) portion of $\text{Re}_2(\text{CO})_8(\mu\text{-H})(\mu\text{-CH=CHC}_4\text{H}_9)_2$ was added to 38.8 mg (0.0661 mmol) of $\text{Au}(\text{PPh}_3)_3$ in 20 mL of hexane. The solution was refluxed for 30 min. After cooling, the solvent was removed in vacuo and the product was isolated by TLC by using hexane solvent to give a yellow band of 3, 65.0 mg (83% yield).

Synthesis of $\text{Re}_2(\text{CO})_8(\mu\text{-I})$, 4, from the reaction of 1 with I_2 . A 6.6 mg (0.026 mmol) portion of I_2 was added to a solution of 20.0 mg (0.0125 mmol) of 1 in 10 mL of benzene. The solution was stirred at room temperature for 15 min. During this time, the solution turned from orange to colorless. The solvent was removed in vacuo, and the residual was separated by TLC by using a 4:1 (v/v) hexane/methylene chloride solvent mixture to give two products in order of elution: (1) a colorless band containing 3.6 mg of $\text{Re}_2(\text{CO})_8(\mu\text{-I})$,¹⁴ 4 (32% yield), and (2) a colorless band of $\text{Au}(\text{PPh}_3)_3$, 4.0 mg (26% yield). Spectral data for 4: IR ν_{CO} (cm^{-1} in methylene chloride): 2107(m), 2030(s), 1997(m), 1960(m). Mass Spec. EI/MS m/z : 850, M^+ .

Reaction of 3 with I_2 . A 3.2 mg (0.0126 mmol) portion of I_2 was added to 30.0 mg (0.0125 mmol) of 3 that was dissolved in 10 mL of benzene. The solution was then stirred for 15 min at room temperature. During this time, the color of the solution turned from yellow to colorless. The solvent was removed in vacuo. The products were isolated by TLC by using a 4:1 hexane/methylene chloride (v/v) solvent mixture to give two products in order of elution: (1) a colorless band that contained 5.0 mg of 4 (23% yield) and (2) a colorless band of $\text{Au}(\text{PPh}_3)_3$, 9.8 mg (66% yield).

Crystallographic Analyses. Red crystals of 1 suitable for X-ray diffraction analyses were obtained from a methylene chloride/hexane solution by slow evaporation of a solvent at 25 °C. Yellow crystals of 3 suitable for X-ray diffraction analyses were obtained from a benzene/octane solution by slow evaporation of a solvent at 15 °C. X-ray intensity data were measured by using a Bruker SMART APEX CCD-based diffractometer by using Mo $K\alpha$ radiation (λ = 0.71073 Å). The raw data frames were integrated with the SAINT+ program by using a narrow-frame integration algorithm.¹⁸ Corrections for Lorentz and

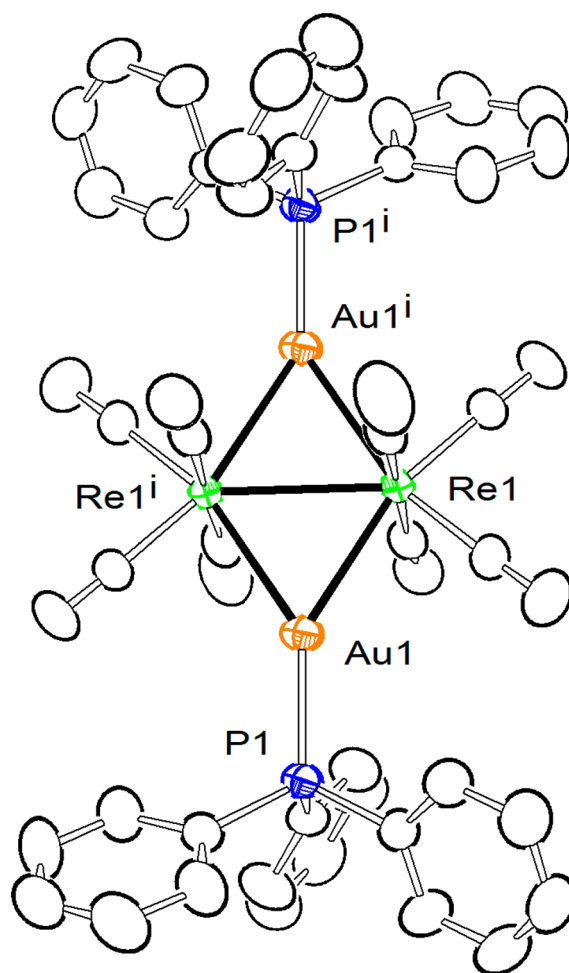


Figure 1. ORTEP diagram of the molecular structure of $\text{Re}_2(\text{CO})_8(\mu\text{-AuPPh}_3)_2$, 1, showing 40% thermal ellipsoid probability. The hydrogen atoms are omitted for clarity. Selected interatomic bond distances (Å) and angles (deg) are as follows: Re1-Au1 = 2.7914(2), Re1-Au1^* = 2.7977(2), Re1-Re1^* = 2.9070(3), Au1-P1 = 2.3308(11); Au1-Re1-Au1^* = 117.320(6), Re1-Au1-Re1^* = 62.681(6), P1-Au1-Re1 = 145.57(3), P1-Au1-Re1^* = 147.68(3).

polarization effects were also applied using SAINT+. An empirical absorption correction based on the multiple measurement of equivalent reflections was applied using the program SADABS. All structures were solved by a combination of direct methods and difference Fourier syntheses, and were refined by full-matrix least-squares on F^2 by using the SHELXTL software package.¹⁹ Crystal data, data collection parameters, and results of the analyses are available in the Supporting Information.

Computational Details. Density functional theory (DFT) calculations were performed with the Amsterdam Density Functional (ADF) suite of programs²⁰ by using the PBEsol functional²¹ with the valence quadruple- ζ + 4 polarization function, relativistically optimized (QZ4P) basis sets for rhenium and gold, the valence triple- ζ + 2 polarization function (TZ2P) basis set for iodine, and double- ζ function (DZ) basis sets for the phosphorus, carbon, oxygen, and hydrogen atoms with nonfrozen cores. The molecular orbitals for 1–4 and $\text{Re}_2(\text{CO})_{10}$ and their energies were determined by geometry-optimized calculations, with scalar relativistic corrections, that were initiated by using the atom positional parameters as determined from the crystal structure analyses. Electron densities at the bond critical points and Mayer bond orders were calculated by using the Bader quantum theory of atoms in molecules (QTAIM) model.^{22,23} Natural bond orbital (NBO) analyses were performed using the GENNBO 6.0 package embedded in ADF 2013.²⁴ Time-dependent DFT (TDDFT) calculations were performed for models in the gas phase by using the PBEsol functional with the same basis sets.

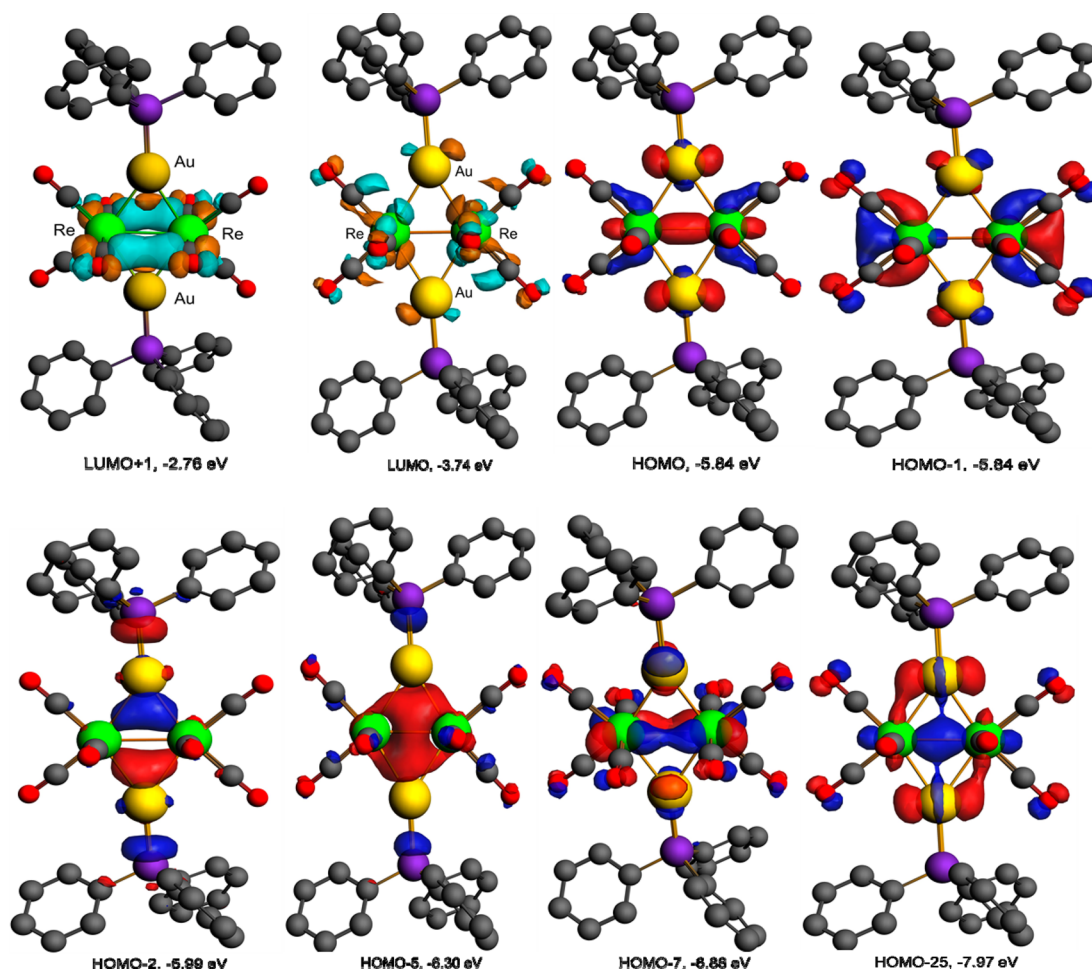
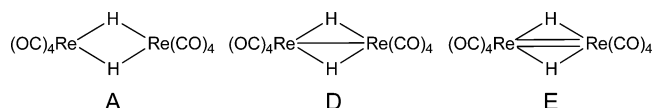


Figure 2. Selected molecular orbital diagrams of the LUMO+1, LUMO, HOMO, HOMO-1, HOMO-2, HOMO-5, HOMO-7, and HOMO-25 (isovalue = 0.04) with calculated energies showing the nature of the bonding in the Re_2Au_2 core of the structure of **1**.

RESULTS AND DISCUSSION

Photolytic decarbonylation of the compound $\text{Re}(\text{CO})_5[\text{Au}(\text{PPh}_3)]$ led to formation of the new complex dirhenium complex $\text{Re}_2(\text{CO})_8(\mu\text{-AuPPh}_3)_2$, **1**, in 18% yield. A coproduct in this reaction was the dirhenium complex $\text{ax,ax-Re}_2(\text{CO})_8(\text{PPh}_3)_2$ ¹⁵ (21% yield). Both compounds were characterized crystallographically. See the Supporting Information for details on the structural analysis of $\text{Re}_2(\text{CO})_8(\text{PPh}_3)_2$. An ORTEP diagram of the molecular structure of **1** is shown in Figure 1. In the solid state, the complex sits on a crystallographic center of symmetry. The molecule contains two $\text{Re}(\text{CO})_4$ groups linked by two bridging AuPPh_3 groups. The two independent Re–Au bond distances, $\text{Re1–Au1} = 2.7914(2)$ Å and $\text{Re1–Au1}^* = 2.7977(2)$ Å, are similar to those found in the compounds $\text{Re}_2(\text{CO})_8[\mu\text{-Au}(\text{PPh}_3)](\mu\text{-C}_2\text{Ph})$,²⁵ 2.744(1) and 2.844(2) Å, and $\text{Re}_2(\text{CO})_8[\mu\text{-Au}(\text{PPh}_3)](\mu\text{-C}_4\text{Fc})$ ²⁶ (Fc = ferrocenyl), 2.7369(3) and 2.8268(3) Å. The Re–Re distance in **1** is 2.9070(3) Å, which is significantly shorter than the Re–Re single bond distance found in $\text{Re}_2(\text{CO})_{10}$: $\text{Re–Re} = 3.041(1)$ Å.²⁷ The dirhenium center in **1** contains only 32 valence electrons and is thus formally unsaturated. Compound **1** is structurally similar to $\text{Re}_2(\text{CO})_8(\mu\text{-H})_2$, **2**, which has two bridging hydrido ligands in the locations of the bridging $\text{Au}(\text{PPh}_3)$ groups of **1**. Compound **2** is also formally unsaturated and has a similarly short Re–Re distance, 2.876(1) Å.⁴ Compound **2** also contains only 32 valence electrons and has been variously described as having no

direct bonding between the two Re atoms,²⁸ A, a Re–Re single bond, D, or a Re–Re double bond, E.^{4b}



Jeiowska-Trzebiatowska et al. analyzed the electronic structure of **2** by using Fenske–Hall (FH) and extended Hückel (EH) methods.²⁸ King reported MPW1PW91 and BP86 geometry-optimized DFT calculations for **2**.²⁹ To investigate the nature of the Re–Re bonding in **1**, we have performed geometry-optimized PBEsol DFT molecular orbital calculations. For the purposes of comparison, we have also performed similar DFT calculations upon **2**; see below.

Selected DFT MOs that show the bonding interactions between the Re and Au atoms in **1** are shown in Figure 2. There is evidence for direct Re–Re bonding in the HOMO, the HOMO-5, and the HOMO-25. The HOMO-5 is a totally symmetric A_g orbital that is dominated by a 4-center bonding interaction that lies principally in the plane of the Re_2Au_2 core of the molecule. The HOMO-2 is dominated by a delocalized 4-center interaction about the Re_2Au_2 core of the molecule with a node along the Re–Re vector. The HOMO-7 provides evidence for a significant d–d π -bonding interaction that lies perpendicular to the Re_2Au_2 plane of the molecule. The low-lying HOMO-25 shows evidence of direct σ -bonding interaction between the two Re atoms.

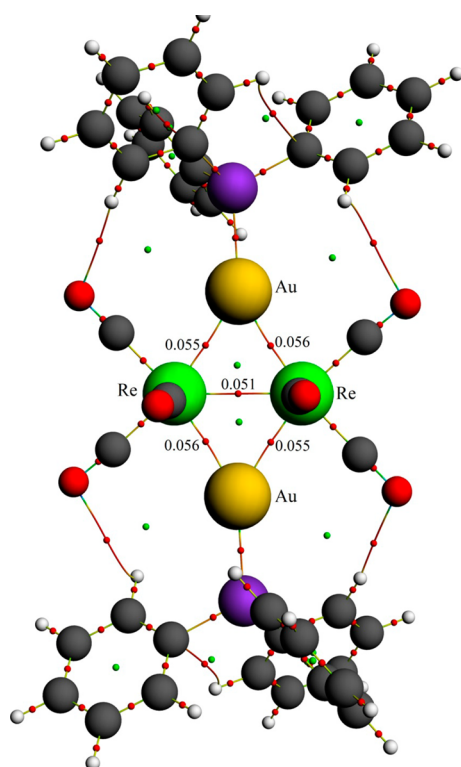


Figure 3. Selected electron densities at bond critical points shown in red calculated by the QTAIM method by using the DFT-optimized structure of **1**.

Figure 3 shows the QTAIM analyzed bond paths about the Re_2Au_2 core and lists the electron densities at selected bond critical points (BCPs) that were obtained from the DFT-optimized structure of **1**. Interestingly, there is a significant electron density of 0.051 e/bohr^3 at the Re–Re BCP. It is almost as large as the electron density at the Re–Au BCPs, 0.055 and 0.056 e/bohr^3 . This supports the idea of a significant direct Re–Re bonding interaction in **1**. Within the framework of the isolobal analogy, $\text{Re}_2(\text{CO})_{10}$ probably provides the best example of a Re–Re σ -type single bond.^{30,31} For comparison, we have similarly calculated the QTAIM electron density at the Re–Re BCP of $\text{Re}_2(\text{CO})_{10}$ by using our PBEsol DFT-optimized analysis. The HOMO of $\text{Re}_2(\text{CO})_{10}$ is consistent with the presence of a strong Re–Re σ -bond; however, the molecular orbital calculations also show that there are two orbitals, HOMO-3 and HOMO-4, that exhibit some supplementary Re–Re π -type bonding interactions; see the Supporting Information. The QTAIM electron density for $\text{Re}_2(\text{CO})_{10}$ at the Re–Re BCP obtained by this calculation was 0.038 e/bohr^3 . A comparison with that of **1** would lead one to the conclusion that the Re–Re bonding interaction in **1** is significantly greater than that in $\text{Re}_2(\text{CO})_{10}$. Indeed, the π -interaction

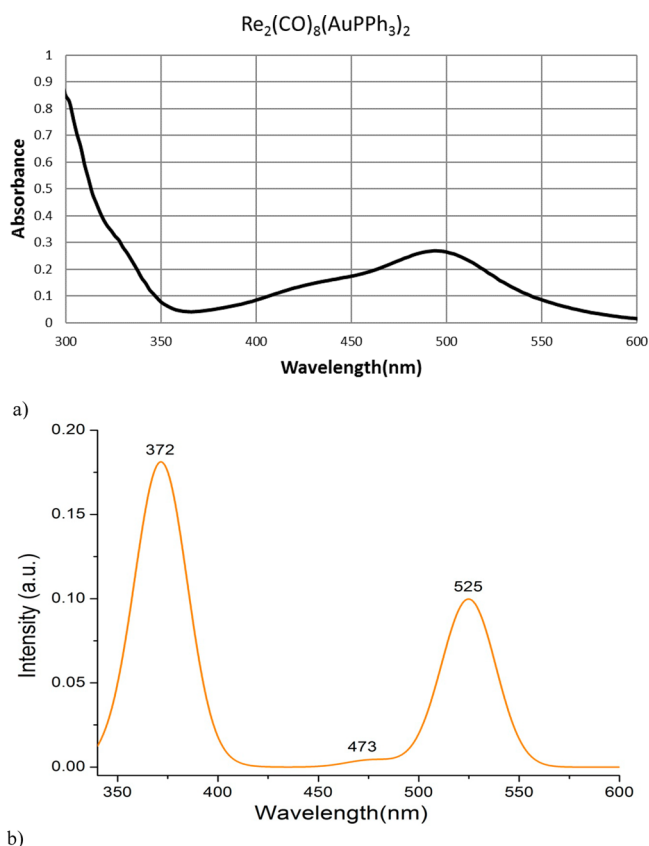


Figure 4. (a) UV–vis absorption spectrum of **1** in CH_2Cl_2 solvent. (b) TDDFT calculated UV–vis absorption spectrum of **1**.

represented in the HOMO-7 of **1** supports the idea of a partial multiple bonding character directly between the two rhenium atoms. To pursue the Re–Re bonding analysis further, we have also performed NBO analyses of **1**. These calculations provided Mayer indices, natural atomic orbitals (NAOs), natural localized molecular orbitals (NLMOs), and a natural population analysis (NPA). These results are presented in Table 1 together with the corresponding results for $\text{Re}_2(\text{CO})_{10}$ and for compounds **2**, **3** and **4**; see below. The Mayer, NAO, NLMO/NPA, and Wiberg indices for **1** are 0.777, 0.192, 0.624, and 0.224, respectively. The corresponding Re–Re values for $\text{Re}_2(\text{CO})_{10}$, 0.264, 0.0324, 0.284, and 0.0922, are all considerably smaller than those of **1**. If we assume that the Re–Re bond order in $\text{Re}_2(\text{CO})_{10}$ is formally 1.0, then it is reasonably concluded that the Re–Re bond order in **1** is greater than 1.0 by all of these measures.

Compound **1** is intensely red in color. Accordingly, a UV–vis spectrum of **1** was obtained. This spectrum is shown in Figure 4a. It exhibits three absorptions in the visible region of the spectrum, $\lambda_{\text{max}} = 327 \text{ nm}$, $\epsilon = 6692 \text{ cm}^{-1} \text{ M}^{-1}$, $\lambda_{\text{max}} = 420 \text{ nm}$,

Table 1. NBO Analyses of the Re–Re Bond Orders Calculated for **1–4** and for $\text{Re}_2(\text{CO})_{10}$

compound	Mayer bond order ^a	NAO bond order ^b	NLMO/NPA bond orders ^b	Wiberg bond index ^c
1	0.777	0.192	0.624	0.224
2	0.522	0.134	0.480	0.180
3	0.457	0.0888	0.319	0.118
4	0.124	-8.8×10^{-3}	1.32×10^{-2}	6.4×10^{-3}
$\text{Re}_2(\text{CO})_{10}$	0.264	0.0324	0.284	0.0922

^aSee ref 34. ^bNAO = natural atomic orbital, NLMO = natural localized molecular orbitals, NPA = natural population analysis. ^cSee ref 35.

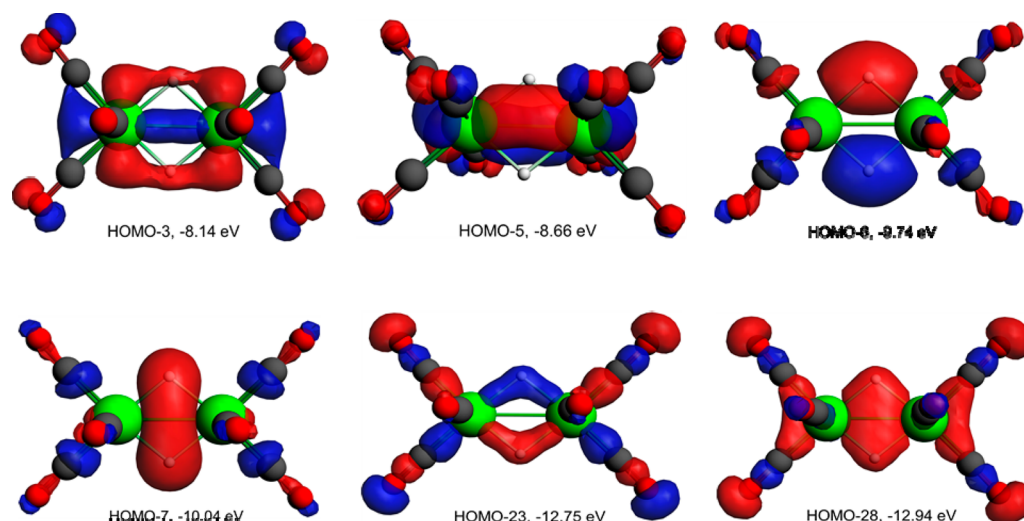


Figure 5. Molecular orbital diagrams of the HOMO-3, HOMO-5, HOMO-6, HOMO-23, and HOMO-28 (isovalue = 0.04) with calculated energies showing the bonding in the Re₂H₂ core of the structure of **2**.

$\epsilon = 2820 \text{ cm}^{-1} \text{ M}^{-1}$, and $\lambda_{\text{max}} = 493 \text{ nm}$, $\epsilon = 5836 \text{ cm}^{-1} \text{ M}^{-1}$, that correlate to electronic transitions between the orbitals in the Re₂Au₂ core of the molecule. A time-dependent DFT (TDDFT) analysis of the electronic transitions has provided the spectrum shown in Figure 4b. The major visible transition at 493 nm (calculated at 525 nm) is attributed to two closely spaced allowed transitions: (1) from the HOMO (74%) and the HOMO-2 (22%) to LUMO ($f = 0.074$) and (2) from the HOMO-2 (75%) and the HOMO (22%) to LUMO ($f = 0.032$). The observed shoulder at 420 nm, calculated to be at 476 nm, is attributed to the HOMO-4 (98%, $f = 0.0043$) to LUMO. The absorption at 327 nm, calculated to be at 372 nm, is attributed to the HOMO-2 (94%, $f = 0.155$) to LUMO+1 transition; see Figure 2 for the MOs.

To compare the influence of the Au(PPh₃) group with H, we have also performed a geometry-optimized DFT analysis of **2**. Selected MOs that focus on the bonding in the Re₂H₂ core of the molecule are shown in Figure 5. The HOMO-3 and HOMO-7 show evidence for direct Re–Re interactions, although they also include substantial overlaps with the two hydrogen atoms. The HOMO-28 is a low-lying symmetric orbital with a significant component delocalized about the Re₂H₂ core, but this orbital also contains significant contributions from the σ -bonding from the four in-plane CO ligands that are largely responsible for its low energy. The HOMO-5 shows that there is significant out-of-plane Re–Re π -bonding as also found in the HOMO-7 in **1**. The HOMO-6 and HOMO-23 show bonding that is predominantly between hydride ligands and the metal atoms. Figure 6 shows the QTAIM analyzed bond paths about the Re₂H₂ core and includes selected electron densities at the BCPs obtained from the optimized structure of **2**. Most interestingly, the electron density along the Re–Re vector (calculated at the ring point of the Re₂H₂ core) is even larger, 0.058 e/bohr³, than that in **1**. The Mayer, NAO, NLMO/NPA, and Wiberg indices for the Re–Re interaction in **2** are similar to those for **1** (see Table 1) and lead to the conclusion that the Re–Re bonding in **2** is also partially multiple in character and very similar to that in **1**. Note: this result differs from the FH and EH analyses performed some years ago, where it was concluded that there is practically no direct M–M bond.²⁸

To investigate the reactivity of **1**, vis-à-vis, its electronic unsaturation, the reaction of **1** with I₂ was performed. When

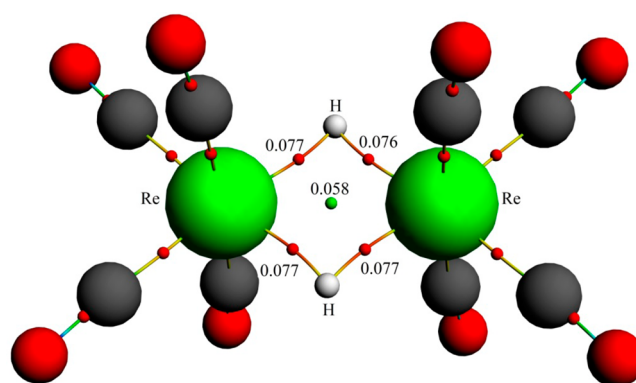


Figure 6. Selected electron densities at bond critical points shown in red and the Re₂H₂ ring point (in green) calculated by the QTAIM method by using the DFT-optimized structure of **2**.

compound **1** was allowed to react with I₂, the new compound Re₂(CO)₈(μ -AuPPh₃)(μ -I), **3**, was obtained in 13% yield. Compound **3** was obtained independently in a much better yield (83%) from the reaction of Re₂(CO)₈(μ -H)(μ -CH=CHC₄H₉) with Au(PPh₃)I. Compound **3** was found to react with I₂ to yield Re₂(CO)₈(μ -I)₂, **4**, in 23% yield. Compound **4** can be obtained directly from **1** in 32% yield by using an excess of I₂.

Compound **3** was characterized by a single-crystal X-ray diffraction analysis, and an ORTEP diagram of the molecular structure is shown in Figure 7. The two rhenium atoms are held together by one bridging AuPPh₃ group and one bridging iodide ligand. The Re–Re bond distance in **3** at 3.1890(12) Å is approximately 0.3 Å longer than that in **1** and 2 and approximately 0.15 Å longer than that in Re₂(CO)₁₀. Because the iodide ligand serves formally as a three-electron donor, the two rhenium atoms in **3** contain a total of 34 valence electrons, and a formal Re–Re single bond is anticipated. This is consistent with the increased length of the Re–Re distance relative to that of **1** and **2**. The Re–Au distances are similar to those found in **1**: Re2–Au1 = 2.7871(9) Å and Re1–Au1 = 2.7935(9) Å. The Re–Re and Re–Au distances in **3** are similar to those observed in the following compounds: Re₂(CO)₈(μ -AuPPh₃)(μ -PPh₂),³² Re–Re = 3.225(2) Å, Re–Au = 2.810(2) and

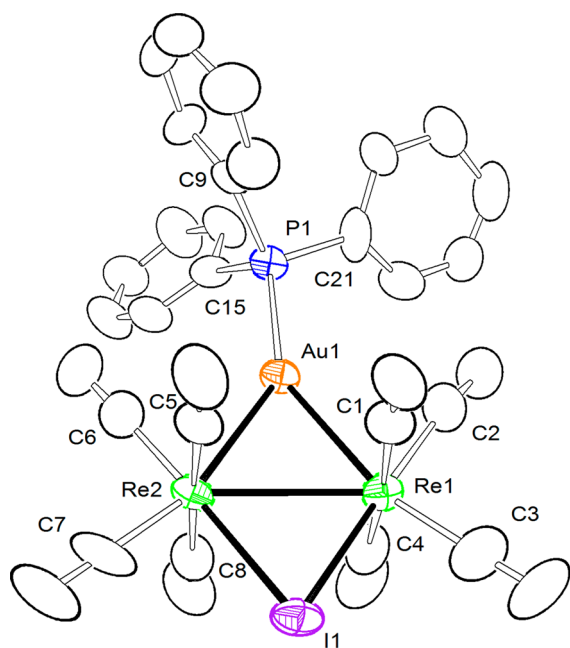


Figure 7. ORTEP diagram of the molecular structure of $\text{Re}_2(\text{CO})_8(\mu\text{-AuPPh}_3)(\mu\text{-I})$, **3**, showing 30% thermal ellipsoid probability. The hydrogen atoms are omitted for clarity. Selected interatomic bond distances (Å) and angles (deg) are as follows: $\text{Re1-Re2} = 3.1890(12)$, $\text{Re2-Au1} = 2.7871(9)$, $\text{Re1-Au1} = 2.7935(9)$, $\text{Re1-I1} = 2.7566(14)$, $\text{Re2-I1} = 2.7845(14)$, $\text{Au1-P1} = 2.322(4)$; $\text{I1-Re1-Au1} = 110.31(4)$, $\text{Au1-Re2-I1} = 109.68(4)$, $\text{Re2-Au1-Re1} = 69.70(3)$, $\text{Re1-I1-Re2} = 70.27(3)$, $\text{Re1-Au1-P1} = 146.92(11)$, $\text{Re2-Au1-P1} = 143.27(11)$.

$2.764(2)$ Å, and $\text{Re}_2(\text{CO})_8(\mu\text{-AuPPh}_3)(\mu\text{-S-2-naphthyl})$,³³ $\text{Re-Re} = 3.1356(7)$ Å, $\text{Re-Au} = 2.27853(8)$ and $2.8110(7)$ Å.³³

The Re-I distances are $\text{Re1-I1} = 2.7566(14)$ Å and $\text{Re2-I1} = 2.7845(14)$ Å, but both are significantly shorter than the distances found in the diiodide complex **4**, $2.827(2)$, $2.826(2)$, $2.813(2)$, and $2.814(2)$ Å, which contains no formal Re-Re bond.¹⁴

NBO analyses of **3** and **4** were also performed; see Table 1. Assuming that the iodide ligand is a three-electron donor and all bonds are of a 2 center–2 electron type, the Re-Re bond order in **3** should be 1. The NBO bond orders for **3** are slightly larger than those for $\text{Re}_2(\text{CO})_{10}$ but smaller than those for **1** and **2**. The QTAIM electron density at the Re-Re BCP in **3** at 0.0357 e/bohr^3 is only slightly larger than that in $\text{Re}_2(\text{CO})_{10}$. Perhaps, the notion of the iodide ligand as a three-electron donor having two 2 center–2 electron σ -bonds to the Re atoms is too simple. Indeed, the HOMO-14, HOMO-15, and HOMO-16 obtained for **3** in our DFT calculations show both delocalized σ - and π -bonding interactions between the iodide ligand and the two rhenium atoms; see Figure 8. The effect of this bonding on the formal Re-Re bond order is difficult to evaluate, but the 3-center σ -bonding of the Re_2I group shown in the HOMO-16 could lead to a slight increase in the electron density at the Re-Re BCP as observed.

Formally, there is no need for the formation of a Re-Re bond in compound **4**. With two bridging iodide ligands serving as three-electron donors, both Re atoms have 18 electron configurations. The observed Re-Re distance in **4** is long at $4.218(2)$ Å¹⁴ and is consistent with the absence of a Re-Re bond. Consistent with this, the Mayer, NAO, NLMO/NPA, and Wiberg indices that were obtained after a geometry-optimized PBEsol MO refinement of the structure of **4** were all close to zero as expected.

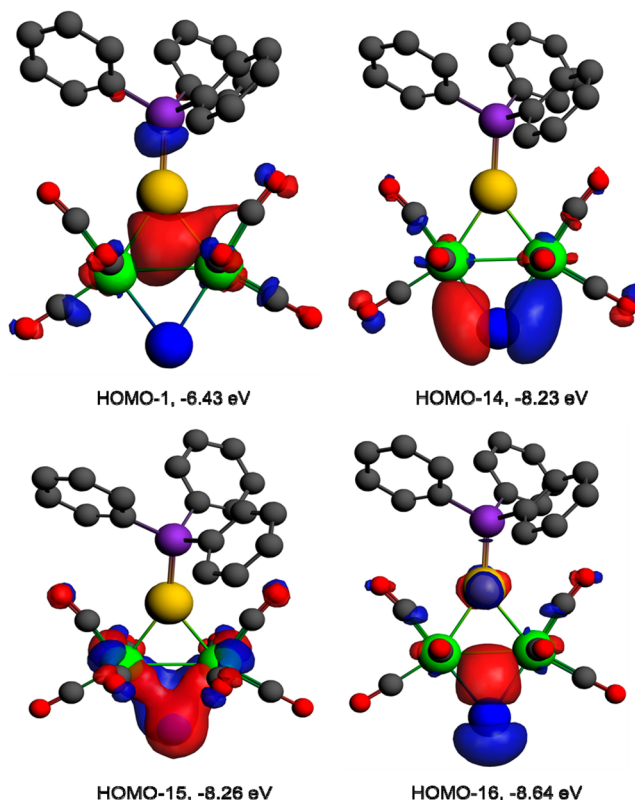
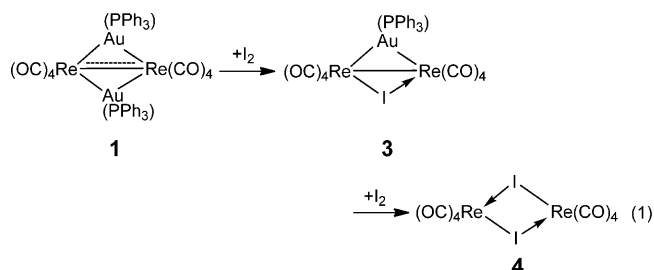


Figure 8. Molecular orbital diagrams of the HOMO-1, HOMO-14, HOMO-15, and HOMO-16 (isovalue = 0.04) with calculated energies showing the bonding in the Re_2AuI core of the molecule of **3**.

SUMMARY AND CONCLUSIONS

The doubly- $\text{Au}(\text{PPh}_3)$ bridged unsaturated complex **1** has been prepared by the photodecarbonylation of $\text{Re}(\text{CO})_5[\text{Au}(\text{PPh}_3)]$. It is assumed that **1** was subsequently formed by the dimerization of two unobserved 16-electron “ $\text{Re}(\text{CO})_4[\text{Au}(\text{PPh}_3)]$ ” groups. Concurrently, the dirhenium complex $\text{ax,ax-Re}_2(\text{CO})_8(\text{PPh}_3)_2$ was formed. This could have been formed by the loss of Au from the incipient “ $\text{Re}(\text{CO})_4[\text{Au}(\text{PPh}_3)]$ ”, followed by the dimerization of two $\text{Re}(\text{CO})_4(\text{PPh}_3)$ radicals. Compound **1** is analogous to the unsaturated, doubly hydride bridged complex **2**. Both compounds possess short Re-Re bond distances. Computational analyses suggest the existence of partial multiple Re-Re bonds in both **1** and **2**. It can be concluded that $\text{Au}(\text{PPh}_3)$ and H have similar effects on the Re-Re bonding in these two compounds. Compound **1** reacts with I_2 to yield the compounds **3** and **4**. This reaction appears to follow the sequence of two steps shown in eq 1. Indeed, we have confirmed independently that **3** does react with I_2 to yield **4**.



The sequential replacement of the bridging one-electron $\text{Au}(\text{PPh}_3)$ groups with three electron-donating bridging iodide

ligands reduces the direct Re–Re bonding present in **1** until it is virtually eliminated in compound **4**.

■ ASSOCIATED CONTENT

■ Supporting Information

Details for the computational analyses of $\text{Re}_2(\text{CO})_{10}$, **1**, **2**, **3**, and **4** and for the structural analyses of **1**, **3**, and $\text{ax,ax-Re}_2(\text{CO})_8(\text{PPh}_3)_2$, including their CIF files, are available. This material is available free of charge via the Internet at <http://pubs.acs.org>.

■ AUTHOR INFORMATION

Corresponding Author

*E-mail: Adamsrd@mailbox.sc.edu.

Notes

The authors declare no competing financial interest.

■ ACKNOWLEDGMENTS

This research was supported by the following grants from the National Science Foundation: CHE-1111496 and CHE-1048629.

■ REFERENCES

- (1) (a) Raubenheimer, H. G.; Schmidbaur, H. *Organometallics* **2012**, *31*, 2507–2522. (b) Stone, F. G. A. *Angew. Chem., Int. Ed. Engl.* **1984**, *23*, 89–99. (c) Evans, D. G.; Mingos, D. M. P. *J. Organomet. Chem.* **1982**, *232*, 171–191.
- (2) (a) Bau, R.; Drabnis, M. H. *Inorg. Chim. Acta* **1997**, *259*, 27–50. (b) Teller, R. G.; Bau, R. *Struct. Bonding* **1981**, *41*, 1–82. (c) Humphries, A. P.; Kaesz, H. D. *Prog. Inorg. Chem.* **1979**, *25*, 145–222.
- (3) (a) Salter, I. D. In *Comprehensive Organometallic Chemistry II*; Abel, E. W.; Stone, F. G. A., Wilkinson, G., Eds.; Pergamon: Oxford, U.K., 1995; Vol. 10, Chapter 5, pp 255–322. (b) Salter, I. D. In *Metal Clusters in Chemistry*; Braunstein, P., Oro, L. A., Raithby, P. R., Eds.; Wiley-VCH: Weinheim, Germany, 1999; Vol. 1, Chapter 1.27, pp 509–534. (c) Salter, I. D. *Adv. Organomet. Chem.* **1989**, *29*, 249–343.
- (4) (a) Bennett, M. J.; Graham, W. A. G.; Hoyano, J. K.; Hutcheon, W. L. *J. Am. Chem. Soc.* **1972**, *94*, 6232–6233. (b) Masciocchi, N.; Sironi, A.; D'Alfonso, D. *J. Am. Chem. Soc.* **1990**, *112*, 9395–9397.
- (5) (a) Broach, R. W.; Williams, J. M. *Inorg. Chem.* **1979**, *18*, 314–319. (b) Churchill, M. R.; Hollander, F. J.; Hutchinson, J. P. *Inorg. Chem.* **1977**, *16*, 2697–2700. (c) Allen, V. F.; Mason, R.; Hitchcock, P. B. *J. Organomet. Chem.* **1977**, *140*, 297–307.
- (6) Wilson, R. D.; Bau, R. *J. Am. Chem. Soc.* **1976**, *98*, 4687–4689.
- (7) Adams, R. D.; Captain, B.; Beddie, C.; Hall, M. B. *J. Am. Chem. Soc.* **2007**, *129*, 986–1000.
- (8) Adams, R. D.; Kan, Y.; Zhang, Q.; Hall, M. B.; Trufan, E. *Organometallics* **2012**, *31*, 50–53.
- (9) (a) Deeming, A. J. *Adv. Organomet. Chem.* **1986**, *26*, 1–96. (b) Keister, J. B.; Shapley, J. R. *J. Am. Chem. Soc.* **1976**, *98*, 1056–1057. (c) Hudson, R. H. E.; Poe, A. J. *Organometallics* **1995**, *14*, 3238–3248.
- (10) Wang, S. R.; Wang, S.-L.; Cheng, C. P. *J. Organomet. Chem.* **1992**, *431*, 215–226.
- (11) Burgess, K.; Johnson, B. F. G.; Kaner, D. A.; Lewis, J.; Raithby, P. R.; Syed-Mustaffa, S. N. A. B. *J. Chem. Soc., Chem. Commun.* **1983**, 455–457.
- (12) Johnson, B. F. G.; Kaner, D. A.; Lewis, J.; Raithby, P. R. *J. Organomet. Chem.* **1981**, *215*, C33–C37.
- (13) Adams, R. D.; Rassolov, V.; Zhang, Q. *Organometallics* **2013**, *32*, 6368–6378.
- (14) Darst, K. P.; Lenhart, P. G.; Lukehart, C. M.; Warfield, L. T. *J. Organomet. Chem.* **1980**, *195*, 317–324.
- (15) Nicholson, B. K.; Bruce, M. I.; bin Shawkataly, O.; Tiekinck, E. R. *J. Organomet. Chem.* **1992**, *440*, 411–418.
- (16) Nubel, P. O.; Brown, T. L. *J. Am. Chem. Soc.* **1984**, *106*, 644–652.
- (17) Westland, A. D. *Can. J. Chem.* **1969**, *47*, 4135–4140.
- (18) SAINT+, Version 6.2a; Bruker Analytical X-ray System, Inc.: Madison, WI, 2001.
- (19) Sheldrick, G. M. *SHELXTL*, Version 6.1; Bruker Analytical X-ray Systems, Inc.: Madison, WI, 1997.
- (20) ADF2013; SCM Theoretical Chemistry, Vrije Universiteit: Amsterdam, The Netherlands. <http://www.scm.com>.
- (21) Perdew, J. P.; Ruzsinszky, A.; Csonka, G. I.; Vydrov, O. A.; Scuseria, G. E. *Phys. Rev. Lett.* **2008**, *100*, 136406.
- (22) (a) Bader, R. F. W. *Atoms in Molecules: A Quantum Theory*; Clarendon: Oxford, U.K., 1990. (b) Cortés-Guzmán, F.; Bader, R. F. W. *Coord. Chem. Rev.* **2005**, *249*, 633–662.
- (23) Keith, T. A. *AIMAll*, Version 12.11.09; TK Gristmill Software: Overland Park, KS, 2012. aim.tkgristmill.com.
- (24) (a) Glendenning, E. D.; Badenhop, J. K.; Reed, A. E.; Carpenter, J. E.; Bohmann, J. A.; Morales, C. M.; Weinhold, F. *NBO 5.0*; Theoretical Chemistry Institute, University of Wisconsin: Madison, WI, 2001. (b) Weinhold, F.; Landis, C. R. *Valency and Bonding: A Natural Bond Order Donor-Acceptor Perspective*; Cambridge University Press: Cambridge, U.K., 2005; pp 32–36.
- (25) Bruce, M. I.; Paul, J.; Low, P. J.; Skelton, B. W.; White, A. H. *J. Organomet. Chem.* **1996**, *515*, 65–79.
- (26) Chedia, R. V.; Dolgushin, F. M.; Smolyakov, A. F.; Lekashvili, O. I.; Kakulia, T. V.; Janiashvili, L. K.; Sheloumov, A. M.; Ezernitskaya, M. G.; Peregudova, S. M.; Petrovskii, P. V.; Koridze, A. A. *Inorg. Chim. Acta* **2011**, *378*, 264–268.
- (27) Churchill, M. R.; Amoh, K. N.; Wasserman, H. J. *Inorg. Chem.* **1981**, *20*, 1609–1611.
- (28) Jeiorska-Trzebiatowska, B.; Nissen-Sobocińska, B. *J. Organomet. Chem.* **1988**, *342*, 215–233.
- (29) Li, N.; Xie, Y.; King, R. B.; Schaefer, H. F., III. *J. Phys. Chem. A* **2010**, *114*, 11670–11680.
- (30) Hoffmann, R. *Angew. Chem., Int. Ed. Engl.* **1982**, *21*, 711–724.
- (31) Xu, B.; Li, Q.-S.; Xie, Y.; King, R. B.; Schaefer, H. F., III. *J. Chem. Soc., Dalton Trans.* **2008**, 2495–2502.
- (32) Haupt, H.-J.; Heinekamp, C.; Florke, U. *Inorg. Chem.* **1990**, *29*, 2955–2963.
- (33) Egold, H.; Schwarze, D.; Flörke, U. *J. Chem. Soc., Dalton Trans.* **1999**, 3203–3207.
- (34) Mayer, I. J. *Comput. Chem.* **2007**, *28*, 204–221.
- (35) Wiberg, K. B. *Tetrahedron* **1968**, *24*, 1083–1096.